Report N00014-76-C-0450-1

⑫ **LEVEL** Ⅲ

A056834 SC

ULTRAVIOLET LASING TRANSITIONS IN DIATOMIC MOLECULES

Joel Tellinghuisen
Department of Chemistry
Vanderbilt University
Nashville, Tennessee 37235

January, 1980

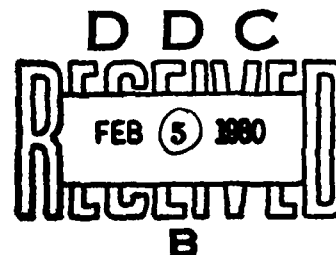Final Report for Period December 1, 1975 to September 30, 1979

Approved for public release; distribution unlimited

D D C

RECEIVED

FEB ⑤ 1980

B

Prepared for

80 2 4 055

# REPORT DOCUMENTATION PAGE

READ INSTRUCTIONS
BEFORE COMPLETING FORM

| 1. REPORT NUMBER | 2. GOVT ACCESSION NO. | 3. RECIPIENT'S CATALOG NUMBER |
|---|---|---|
| N00014-76-C-0450-1 | | Final rept. 1 Dec 75-30 Sep 79 |

4. TITLE (and Subtitle)

ULTRAVIOLET LASING TRANSITIONS IN DIATOMIC MOLECULES.

5. TYPE OF REPORT & PERIOD COVERED

FINAL (12/1/75 - 9/30/79)

6. PERFORMING ORG. REPORT NUMBER

7. AUTHOR(s)

Joel Tellinghuisen

8. CONTRACT OR GRANT NUMBER(s)

N00014-76-C-0450 DARPA Order-2840

9. PERFORMING ORGANIZATION NAME AND ADDRESS

Joel Tellinghuisen
Department of Chemistry, Vanderbilt University
Nashville, Tennessee 37235

10. PROGRAM ELEMENT, PROJECT, TASK AREA & WORK UNIT NUMBERS

DARPA Order No. 2840/10
Program Code 8E20

11. CONTROLLING OFFICE NAME AND ADDRESS

Defense Advanced Research Projects Agency
1400 Wilson Boulevard
Arlington, Virginia 22209

12. REPORT DATE

January 1980

13. NUMBER OF PAGES

30    12  30

14. MONITORING AGENCY NAME & ADDRESS(If different from Controlling Office)

Physics Program, Physical Sciences Division
Office of Naval Research
800 N. Quincy Street, Arlington, VA 22217

15. SECURITY CLASS. (of this report)

Unclassified

15a. DECLASSIFICATION/DOWNGRADING SCHEDULE

16. DISTRIBUTION STATEMENT (of this Report)

Approved for public release; distribution unlimited.

17. DISTRIBUTION STATEMENT (of the abstract entered in Block 20, if different from Report)

18. SUPPLEMENTARY NOTES

19. KEY WORDS (Continue on reverse side if necessary and identify by block number)

UV lasers, rare gas halide spectroscopy, halogen spectroscopy, Franck-Condon factors, emission spectroscopy, tesla discharge

20. ABSTRACT (Continue on reverse side if necessary and identify by block number)

The work performed under this contract is primarily directed toward a better spectroscopic understanding of UV laser transitions in selected diatomic molecules. Specifically the work emphasizes the analysis of spectroscopic data for discrete (bound-bound) and diffuse (bound-free) transitions in the rare gas monohalide (RgX) molecules, and discrete transitions in the homonuclear halogens. The primary accomplishments of the work include (1) detailed rotational and vibrational analyses of the lasing B→X transition in

DD FORM 1473  EDITION OF 1 NOV 65 IS OBSOLETE
1 JAN 73
S/N 0102-LF-014-6601

363  825

XeF (3500 A) and the lasing $D' \to A'$ transition in $Br_2^n$ (2900 A); (2) vibrational analyses of the lasing transitions $B \to X$ in XeCl (3100 A) and $D' \to A'$ in $I_2$ (3400 A), and the nonlasing $D \to X$ transitions in XeF (2600 A) and XeCl (2350 A); (3) analysis of the bound-free $B \to X$ and $D \to X$ transitions in other RgX molecules, with emphasis on KrCl; (4) reanalysis of the $D \to X$ UV fluorescence spectrum of $I_2^n$; (5) determination of potential curves and intensity factors (Franck-Condon factors, stimulated emission cross sections) for all analyzed systems; (6) determination of the energy ordering of the B and C states in KrCl, XeCl, and XeBr, using temperature-dependent emission spectroscopy; and (7) characterization of a tesla discharge with respect to its temporal and thermal properties and its total radiant output. These studies are of relevance to the better understanding of these new lasers and to the development of more complete and correct mathematical models for describing and predicting their performance.

## I. INTRODUCTION

Beginning in 1975 workers in several laboratories have developed a new class of lasers which operate on transitions in the diatomic noble gas halide (RgX) molecules. Specifically, lasing has been achieved for XeBr (2820 A),[1] XeCl (3080 A),[2a] XeF (3510 and 3530 A),[2b,3a] KrCl (2220 A),[4a] KrF (2490 A),[2a,5a] ArCl (1750 A),[6] and ArF (1930 A).[5b] In similar experiments lasing has also been reported for UV transitions in $I_2$ (3420 A),[2c,3b] $Br_2$ (2920 A),[4b] $F_2$(1580 A),[5c] and $Cl_2$ (2580 A).[5d] Since the initial reports, dozens of papers have been published on these new lasers, and they are now available commercially. The RgF lasers have been made to operate with moderate efficiency (1-3%) and high pulse power ($10^9$ W), hence are of possible practical import in laser isotope separation schemes and military applications. All of these new lasers hold promise as laboratory research tools.

The work in our laboratory has been directed toward a better understanding of the spectroscopy of these new electronic transition lasers, through analysis and interpretation of experimental spectra. The primary results of the analyses are potential curves for the various electronic states and intensity factors descriptive of the spontaneous emission probabilities and the stimulated emission cross sections. In the course of this work we have also characterized in detail the tesla discharge we use to generate our experimental spectra. Specifically we have investigated the thermal and temporal properties of the discharge as functions of pressure, composition, and wall temperature.

## II. RESEARCH PROGRESS

### A. Rare Gas Halides

### 1. Overview

Our work has largely supported the early qualitative descriptions of the lasing transitions in the RgX molecules. That is, the excited state which gives rise to lasing indeed appears to be the lowest ionic state (however, see below), and this state has a potential curve that approximates the ground state potential for the analogous alkali halide molecule (e.g. XeCl ↔ CsCl). The RgX lasing transition terminates on the ground state, which in every case but one (XeF)[7] has a relatively "flat" potential curve in the Franck-Condon region. In all but two cases (XeF, XeCl)[7] the transition is mainly bound-free for all

vibrational levels of the emitting state; however, because of the flatness of the lower potential curve the spectrum bunches up in a narrow (~100 A) wavelength region and displays some "vibrational" structure in all cases.

The potential diagram for each RgX molecule is similar to that shown for XeBr in Fig. 1.[7c] The lasing state is now commonly called the B state by experimentalists. Simple considerations suggest that both this state and the
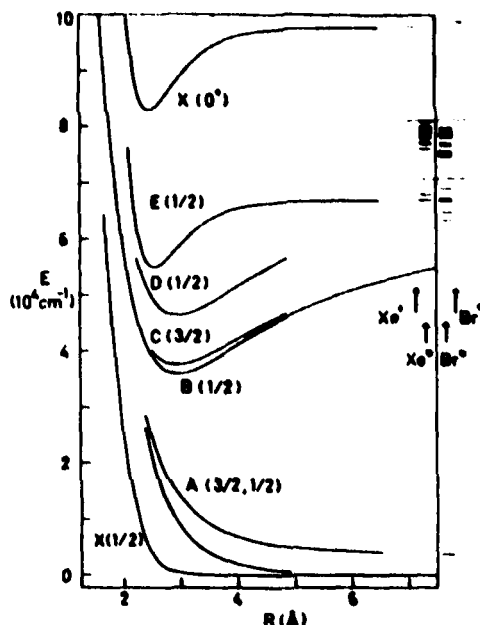


FIG. 1. Potential diagram for XeBr. The $B$ and $X$ curves are based on results of this study; the other curves are only qualitatively correct (see text). The $X$ curve of XeBr is drawn as the $X$ curve of IBr. Low-lying states of Xe*, Xe*, Br*, and Br* are shown to the right. The ion-pair energies, Xe*($^1P_{3/2, 1/2}$) + Br*, are indicated by the two longer lines; the $B$ and $C$ curves go to the lower of these and the $D$ curve to the upper.

ground state should be of $^2\Sigma^+$ symmetry. However, detailed theoretical calculations[8] and work on the rotational structure of XeF[9] both indicate that the B state displays strong tendencies toward Hund's case (c) coupling. In the fluorides the ground state appears to be a good Hund's case (b) $^2\Sigma^+$ state. However, it too may show case (c) tendencies in the heavier halides. In any event the B → X lasing transition owes its intensity to its $^2\Sigma^+$ - $^2\Sigma^+$ character. The C state lies much closer to B than depicted in Fig. 1. In fact there is strong evidence that C lies lower than B in XeF[10-12], but recent temperature

dependence studies place C slightly above B in most of the other RgX molecules.[13] The C state has not been well characterized spectroscopically for any of the RgX molecules, because it has not been observed in any transitions which display appreciable structure. Its radiative decay occurs mainly to the un-bound A state. Like the B state, the D state is a case (c) mixture of $^2\Sigma^+$ and $^2\Pi$, with strongest radiative decay to the X state. Analyses of the vibrational structure in the D $\to$ X systems of XeF[9] and XeCl[14] indicate that in both molecules the D state is slightly deeper (larger $\mathcal{D}_e$) than the B state, with a larger vibrational frequency and smaller internuclear distance. The state labeled E in Fig. 1 represents the lowest bound Rydberg state. This state is expected to resemble the ground state of the appropriate RgX$^+$ ion, which in turn should approximate in a crude sense the isoelectronic ground state of the analogous molecule (e.g. XeBr$^+$ $\leftrightarrow$ IBr). Hence the E state should have a smaller $\mathcal{D}_e$ and $R_e$ but a larger $\omega_e$ than the ionic (B,C,D) states. The low-lying Rydberg states have not yet been observed experimentally, except possibly in transient absorption in the laser spectrum of KrF.[15]

The approximate validity of the alkali halide model[16,17] for describing the ionic states of the RgX molecules in illustrated in Table I. The B-state vibrational frequencies and $\mathcal{D}_e$ values are about 90% of the values for the cor-responding alkali halide X states. The $R_e$ values are known experimentally in only two cases -- the B and D states of XeF. The other values in Table I are simply predictions from the truncated Rittner potential employed in the analyses.[7,9,14] For XeF the Rittner model underestimates $R_{eB}$ and $R_{eD}$ by 0.06 A and 0.01 A, respectively. The Rittner predictions for $R_{eB}$ are uniformly smaller (by 0.1-0.3 A) than the ab initio theoretical predictions,[8] so in general the true $R_{eB}$ values are probably slightly larger than the corresponding $R_{eX}$ (alkali halide) values. In XeF and XeCl the D states are deeper, stiffer, and shorter than the B states, hence more closely resemble the corresponding alkali halide X states. In KrCl the differences between the B and D states are considerably less than in XeF and XeCl.[18] In the ArX molecules the B/D electronic splitting is much smaller than in the KrX and XeX molecules, so the differences in the structural constants for the B and D states are expected to be still further reduced.

In all of the RgX molecules except XeF the ground state appear to be bound mainly by dispersion type interactions, although configuration mixing with the ionic $^2\Sigma^+$ state lowers these curves appreciably from their otherwise

TABLE I. Comparison between ion-pair excited states of the rare gas halides and ground states of the corresponding alkali halides (units $cm^{-1}$ and A).[a]

| | $\omega_e$[b] | $\omega_e x_e$[c] | $R_e$[c] | $D_e$ (ions) |
|---|---|---|---|---|
| XeF(B) | 309 | 1.51[1.33] | 2.63[2.57] | 42,780 |
| XeF(D) | 350 | 1.90[1.80] | 2.51[2.50] | 44,080 |
| CsF(X) | 353 | 1.62 | 2.35 | 45,660 |
| $Xe^{35}Cl(B)$ | 195 | 0.63[0.64] | [3.01] | 36,550 |
| $Xe^{35}Cl(D)$ | 204 | 0.68[0.72] | [2.92] | 37,150 |
| $Cs^{35}Cl(X)$ | 214 | 0.74 | 2.91 | 39,300 |
| XeBr(B) | 120(10) | [0.23] | [3.03] | 34,700 |
| $Cs^{79}Br(X)$ | 150 | 0.36 | 3.07 | 38,000 |
| XeI(B) | 112(8) | [0.24] | [3.38] | 32,920 |
| CsI(X) | 119 | 0.25 | 3.32 | 35,380 |
| KrF(B) | 310(20) | [1.20] | [2.33] | 44,670 |
| RbF(X) | 373 | 1.80 | 2.27 | 46,750 |
| KrCl(B) | 215(7) | [0.75] | [2.85] | 37,900 |
| KrCl(D) | 215(10) | [0.76] | [2.81] | 37,900 |
| $Rb^{35}Cl(X)$ | 233 | 0.86 | 2.79 | 39,680 |

[a] Values for alkali halides from Brumer and Karplus [J. Chem. Phys. 58, 3903 (1973)].

[b] Estimated standard errors in parentheses. Where not given the errors are within the precision of the last digit.

[c] Values in brackets predicted by truncated Rittner model.

expected positions.[8] As a result of such mixing the X state of XeCl is bound by 280 $cm^{-1}$, which is more than twice the value for the nearest "true" van der Waals molecule (XeAr); and the internuclear distance is shorter by 1 A. In all other RgX molecules (save XeF) only diffuse (bound-free) B → X and D → X emission has been observed. This indicates that in these cases the bound portion of the X-state well lies outside the Franck-Condon region for transitions from the low v' levels which are mainly responsible for the emission at moderate-to-high pressures (P > 50 torr). In other words the combined effects of dispersion forces and configuration mixing fail to pull the X-state well in on the R axis sufficiently to make discrete emission observable in all the RgX molecules except XeCl and XeF. However these forces do yield X curves which are only gently repulsive near $R = R_{eB}$. Consequently the emission concentrates in a relatively narrow spectral region and displays analyzable structure.

The B → X and D → X spectra of all the RgX molecules except XeF bear a qualitative resemblance to the XeBr B → X spectrum illustrated in Fig. 2. As shown in Fig. 3, the origin of the structure is the inherent reflection character in the contributions from the individual v' levels, which persists in the thermally averaged spectrum. The near coincidence of the red-most peaks for the different v' levels is ascribable to a minimum in the difference potential, $U_B(R) - U_X(R)$, and is important for the lasing potential of these molecules, because it means that all excited molecules can lase at a common wavelength.

The X state of XeF is anomalous.[9,19] In this case the dispersion interactions and configuration mixing are strong enough to produce an appreciably bound state ($D_e = 1200$ $cm^{-1}$) with an internuclear distance smaller than $R_{eB}$ and $R_{eD}$. The XeF B → X spectrum is a complex overlap of v'-v" bands, some red-degraded, some violet-degraded, and many displaying both red- and violet-degraded features. The occurrence of such complex structure is due in part to the great anharmonicity of the X state, which makes its rotational and distortional constants strongly v" dependent, and in part to the mixed coupling situation (case (c) upper, case (b) lower state). The D → X spectrum of XeF is similarly complicated, but still significantly different, because of a different spin coupling constant and smaller internuclear distance in the D state.

## 2. Single Isotope Studies of XeF and XeCl

Previous work on the discrete structure in the spectra of XeCl and XeF has been hindered by isotopic blending arising from the large number of isotopes
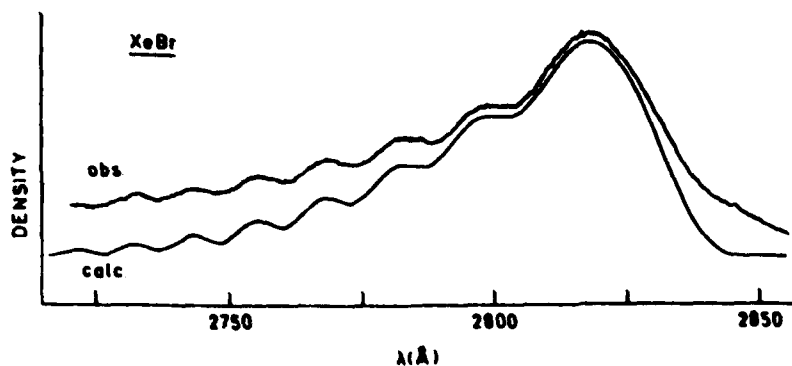
FIG. 2. Experimental spectrum (microdensitometer tracing) and final simulated spectrum for $B - X$ transition in XeBr . The latter was calculated using the potential parameters of Table I and $J' = J''$ = 71. For calibration the peaks near 2820, 2780, and 2740 Å in the calculated spectrum have intensities in the ratio 100/24/4, 9.
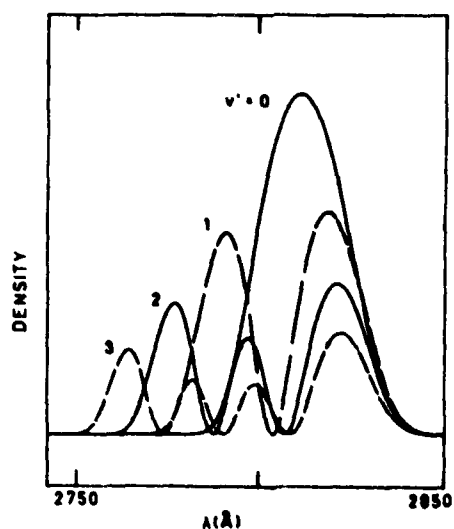


FIG. 3. Decomposition of XeBr spectrum of Fig. 2, showing contributions from $v' = 0$, 1, 2, and 3.

in natural Xe.  In the case of XeF it was possible to rotationally analyze a single band (the 1-2 band) in the B-X system, where there is a fortuitous cancellation of the vibrational isotope shifts.[9]  From this one band it was possible to estimate internuclear distances and derive approximate potential curves for the X, B and D states.  However the derivation relied on several somewhat speculative assumptions.  To put the analysis on firmer footing, we have been carrying out a detailed analysis of the B-X spectrum of the single isotopic molecule $^{136}Xe^{19}F$.

The XeF emission is readily produced in a tesla discharge through a gas mixture containing 1 torr $SF_6$, 2 torr $^{136}Xe$ (95% isotopically pure), and 100-600 torr Ar.  To minimize collisional broadening of the rotational lines, we use Ar pressures below 150 torr.  The spectra are recorded photographically at a resolution of 150,000-200,000.

To date we have rotationally analyzed 11 bands in the B-X system spanning v' levels 0-4 and v" levels 0-5.  The constants obtained in this band-by-band analysis are summarized in Table II.  We hope to extend the analysis to include v' levels 5 and 6 and v" levels 6 and 7 before terminating our work on this system.  The analysis confirms the previous work[9] qualitatively but yields slightly different spectroscopic constants.  For the B state we give the following preliminary expressions for the rotational and vibrational constants (valid for $^{136}Xe^{19}F$):

$$B_v = 0.14564 - 7.5 \times 10^{-4}(v+\tfrac{1}{2}) \tag{1}$$

$$G_v = 308.16(v+\tfrac{1}{2}) - 1.496(v+\tfrac{1}{2})^2 \tag{2}$$

From the value of $B_e$ in Eq. (1) the internuclear distance in the B state is calculated to be $R_e = 2.6353(5)$ A (cf. 2.631 A estimated previously).

To obtain expressions for $B_v$ and $G_v$ for the X state, of reliability comparable to that of Eqs. (1) and (2), it will be necessary to do a correlated least-squares fit of the band-by-band results.  We hope to complete this calculation soon and use the results to identify the specific transitions prominent in the laser spectrum of "natural" XeF.[20]  In the absence of these more precise results, we can still make some comparisons with the previous[9] constants for the X state.  The new ΔG" values agree with those calculated from the previous constants within 0.25 $cm^{-1}$ for v" = 0-5; and the $B_v$ values agree with the previous values within $1 \times 10^{-4}$ $cm^{-1}$ for v" = 2-4 but are about $5 \times 10^{-4}$ $cm^{-1}$ lower for v" = 1 and 5, and $16 \times 10^{-4}$ $cm^{-1}$ lower for v" = 0.  The changes in the

TABLE II. Spectroscopic constants from band-by-band rotational analysis of B → X spectrum of $^{136}Xe^{19}F$. All quantities are given in cm$^{-1}$. Constants are as defined in Ref. 9b.

| v'-v" | $\nu_0$ | B' | B" | D"x10$^7$ | δ | α | bx10$^{10}$ | σ |
|---|---|---|---|---|---|---|---|---|
| 1-2 | 28773.877(10) | 0.14470(6) | 0.17510(7) | 9.63(17) | 1.86851 | -0.08319 | -2.45 | 0.035 |
| 2-1 | 29259.121(8) | 0.14377(4) | 0.18162(5) | 7.78(13) | 1.80826 | -0.03660 | -4.32 | 0.023 |
| 1-1 | 28956.942(9) | 0.14454(5) | 0.18163(6) | 7.97(14) | 1.78788 | -0.01780 | -3.47 | 0.031 |
| 0-5 | 28055.618(34) | 0.14529(15) | 0.14679(17) | 18.72(43) | 1.73771 | 0.02467 | -4.18 | 0.042 |
| 0-4 | 28169.789(13) | 0.14528(9) | 0.15797(10) | 15.25(20) | 1.81447 | -0.05109 | -3.23 | 0.029 |
| 0-1 | 28651.772(8) | 0.14524(5) | 0.18159(5) | 7.98(14) | 1.83061 | -0.04729 | -0.84 | 0.029 |
| 0-3 | 28307.600(8) | 0.14531(4) | 0.16717(5) | 11.96(13) | 1.83237 | -0.04928 | -5.06 | 0.022 |
| 0-2 | 28468.711(12) | 0.14520(5) | 0.17484(6) | 9.61(16) | 1.87715 | -0.07982 | -4.54 | 0.029 |
| 4-0 | 30058.083( ) | 0.14217(6) | 0.18737(6) | 6.74(11) | 1.79692 | -0.05634 | 6.20 | 0.034 |
| 4-1 | 29854.478( ) | 0.14235(5) | 0.18163(5) | 7.41(9) | 1.86692 | -0.10819 | 5.61 | 0.031 |
| 2-0 | 29462.708( ) | 0.14377(7) | 0.18740(8) | 6.58(22) | 1.80399 | -0.03391 | -8.77 | 0.034 |
| 4-4 | 29372.492(27) | 0.14235(6) | 0.15823(8) | 16.43(19) | 1.79715 | -0.07644 | 2.58 | 0.033 |
| 3-3 | 29214.109(14) | 0.14274(7) | 0.16681(7) | 11.44(14) | 1.81442 | -0.05032 | 1.58 | 0.031 |

$B_v$" curve imply changes in the X-state potential curve and corresponding changes in the FCFs. The new estimate of $R_e$" is 2.31 A, or 0.02 A larger than the previous value.

The spin splitting constants $\alpha$ and $\delta$ are the most elusive parameters in the analysis, as indicated by the amount of "play" in the estimates of these constants in the band-by-band analyses. Here particularly the correlated LS fit will be required to pin down the constants reliably. As in the previous work[9] we observe anomalous behavior in the LS fits when transitions having large rotational quantum numbers (N > 50) are included in the fits. These anomalies are tentatively attributed to interaction with the C state but have not yet been quantitatively interpreted.

Single isotope spectra have also been recorded and analyzed for XeCl ($^{136}Xe^{35}Cl$). However, because of the large reduced mass and the small vibrational frequency in the ground state of XeCl, rotational structure could not be resolved well enough for analysis. The results of this work have been published in full[14] and were reviewed in the preceding section of this report, so will not be discussed further here.

### 3. Bound-Free RgX Emission

As was noted earlier, of all the RgX molecules only XeF and XeCl display clear discrete structure in their emission spectra. Nevertheless the structure in the bound-free B $\rightarrow$ X and D $\rightarrow$ X systems of most of the other RgX species is amenable to quantitative analysis through computer simulation of the observed spectra. In early work on such spectra, we were able to determine approximate B and X potential curves for KrF, XeBr, and XeI.[7c] However that work suffered from several minor deficiencies, which may have led to slight systematic errors in the results: (1) Spectra were recorded at a single pressure, which in at least two cases was probably not sufficiently high to ensure the Boltzmann vibrational population distributions assumed in the spectral simulations. (2) There was uncertainty about the heavy-body temperature of the e-beam-produced discharge. (3) The spectra were recorded on film, which was intensity calibrated under conditions sufficiently different from those of the discharge (i.e. different source wavelength distribution and temporal behavior) as to have possibly introduced errors into the calibration. (4) In the spectral computations a constant dipole strength function $|\mu_e|^2$ was assumed, whereas theoretical work[8] indicates that $\mu_e$ can vary significantly with internuclear distance over even the narrow region of R sampled by the emission from low v' levels.

To remedy these deficiencies we have carried out more extensive studies of the RgX bound-free emissions, in which we have (1) worked at known source temperatures, (2) varied the total pressure to permit extrapolation to infinite P, (3) recorded spectra photoelectrically, and (4) allowed for a variation in $\mu_e$ with R in the spectral simulations. Most of this work has been concentrated on the KrCl molecule, both its B → X and its D → X systems.[18] We have also recorded spectra for KrF, ArF, ArCl, and XeI, but have done little analysis in these cases.

Figure 4 illustrates the pressure dependence of the intensities of the first few long-wavelength peaks in the B → X spectrum of KrCl, as studied in Ar buffer.
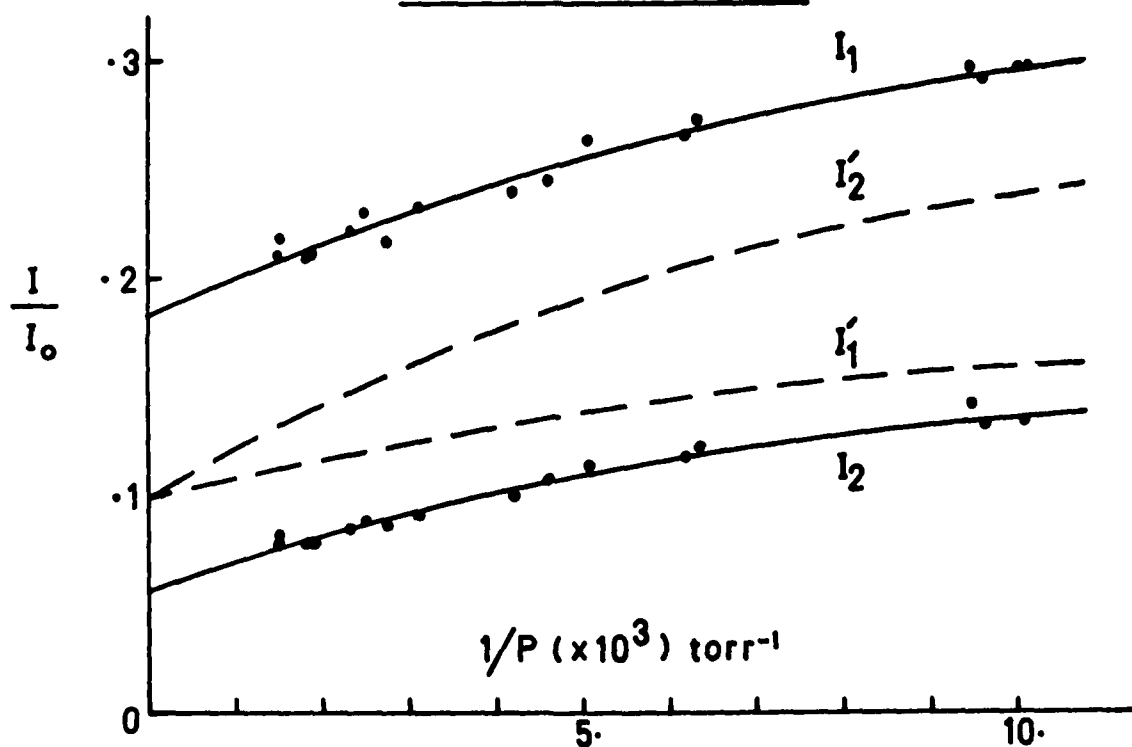


Fig. 4.  Relative intensities of the first and second peaks to the blue of the main peak in the B→X spectrum of KrCl, as functions of Ar buffer pressure. Curves marked $I_1'$ and $I_2'$ show the same data normalized to a common intercept.

(The spectrum itself is illustrated below in Fig. 5.)  Only relative intensities were recorded, as the absolute intensity varies in a more complex manner with the conditions of the discharge.  To obtain the infinite P intercepts, the relative intensities were fitted to low-order polynomials

in 1/P. From a comparison of the intercepts obtained from different-order
fits, and from the standard errors themselves, we conclude that we can determine
the infinite P ratios within 3-10% -- except for emission in a He buffer,
where vibrational relaxation is far from complete at the highest P we can
achieve in our discharge (1 atm). We expect also to be able to determine
approximate vibrational relaxation rates, but have not done so yet.

Figures 5 and 6 illustrate typical B → X and D → X spectra recorded for
KrCl; the final computer-simulated spectrum is included in Fig. 5. From
this analysis we find $\omega_{eB}$ = 215±7 cm$^{-1}$ and concluded that $|\mu_e|^2$ declines with
increasing R in the Franck-Condon region, but not as rapidly as suggested by
an extrapolation of the theoretical results for other RgX molecules.[8] The
analysis of the D → X system is not yet complete; but a comparable value of
$\omega_{eD}$ = 215 ± 10 cm$^{-1}$ is indicated, and there appears to be a slight increase
in $|\mu_e|^2$ with R. Also, unlike the XeX cases, the dissociation energies in
the B and D states appear to be nearly identical. And the difference in $R_e$
for the B and D states is smaller than observed for XeCl and XeF (0.04 A
compared with 0.09 A in XeCl and 0.12 A in XeF).

### 4. Energy Ordering of the B and C States

Theoretical calculations[8] indicate that the B and C(3/2) states are nearly
degenerate near their potential curve minima, making it possible that the
energy ordering of these states may be the reverse of their alphabetic labeling.
In fact experimental evidence is strongly supportive of a reversed ordering
in XeF,[10-12] and a similar reversal has been suggested for the other rare gas
fluorides and chlorides.[11] However, these results are based on a comparison
of the total B → X and C → A emission intensities at a single temperature,
interpreted with the theoretical transition strength ratios. If the latter
are in error, the derived B/C energy separations could be off by enough to
alter the estimated ordering.

To help resolve the issue we have investigated the temperature dependence
of the C-A/B-X intensity ratio in KrCl, XeCl, XeBr, and XeI. Typical spectra
recorded for KrCl and XeBr at 360 K and 800 K are illustrated in Figs. 7 and 8.
Careful comparisons of the total emission in the broad band with that in the
narrow B → X peak show that the (broad-band)/(B → X) ratio increases with
increasing T for KrCl but decreases slightly for XeCl and XeBr. These results
imply that the C state lies higher than the B state in KrCl but lower in XeCl and
XeBr. We are currently trying to estimate the C/B separations and the C → A/
B → X spontaneous emission ratios from these data, but the determination is

KrCl B→X
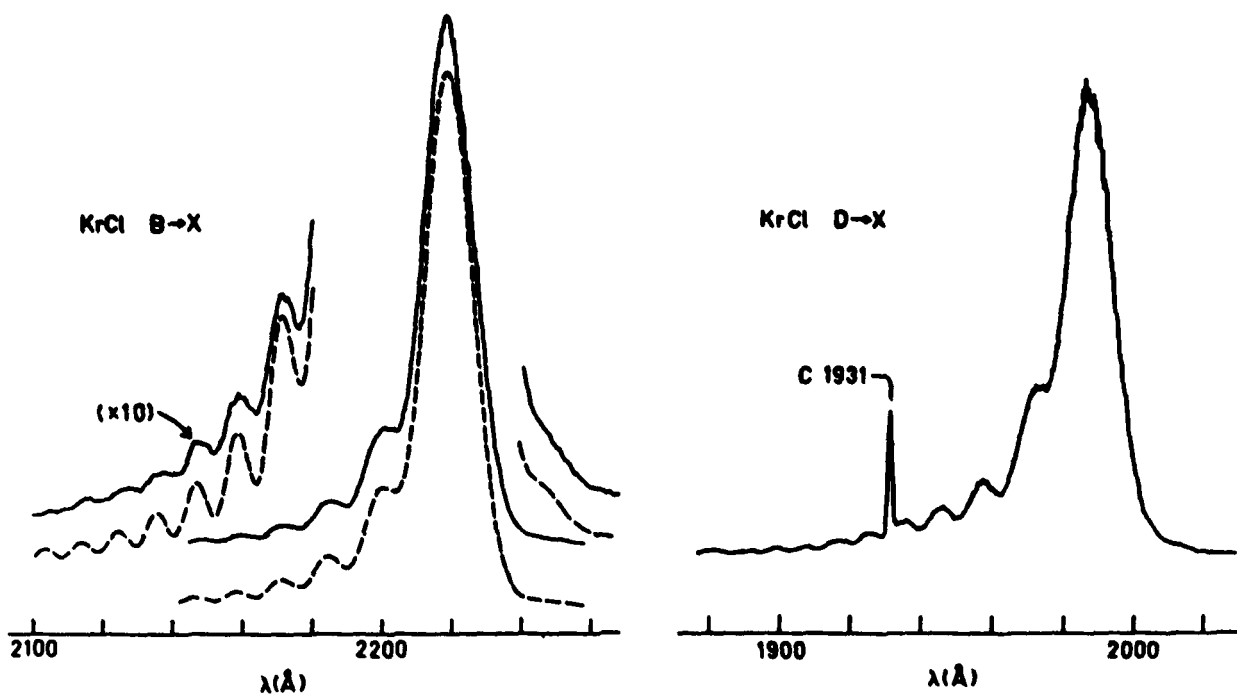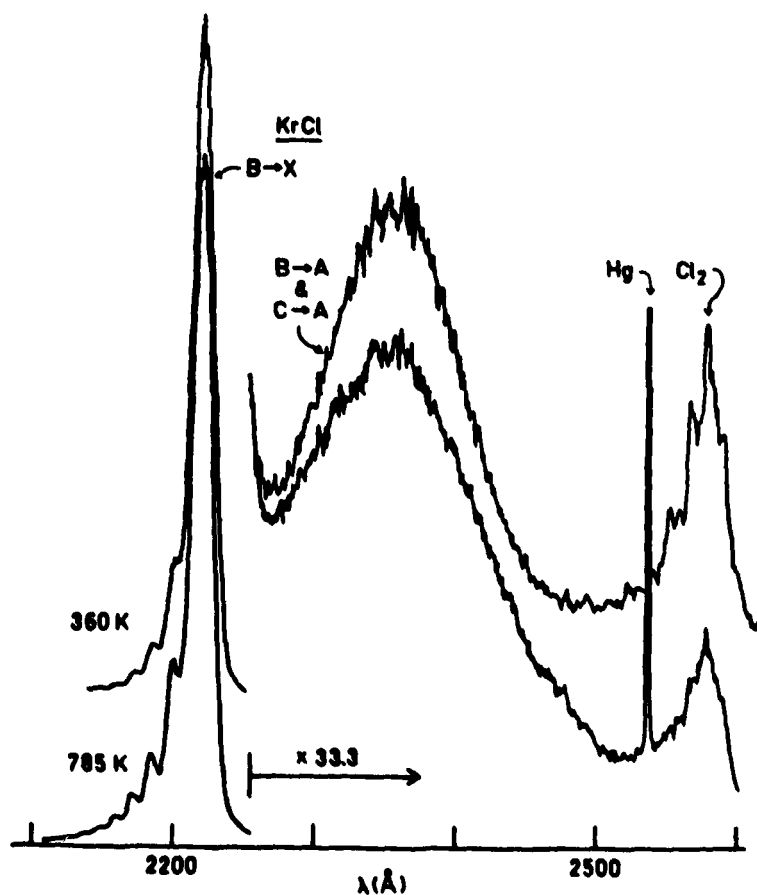
(×10)

2100 2200

λ(Å)

KrCl D→X

C 1931

1900 2000

λ(Å)

Fig. 5. Experimental (upper) and calculated spectra for the B→X transition in KrCl.

Fig. 6. Experimental spectrum of the D→X transition in KrCl.

Fig. 7. Experimental emission spectra of KrCl recorded at two temperatures, showing the broad-band emission (B→A & C→A) and the B→X system.

KrCl

B→X

B→A
&
C→A

Hg

Cl₂

360 K

785 K

× 33.3

2200 2500

λ(Å)

complicated by the considerable overlap of the C → A and B → A emissions in the broad band. The latter transition has significant intensity in the non-fluoride RgX molecules, and the overlap is particularly bad for the chlorides. Thus the estimate of $\Delta\varepsilon = T_{eC} - T_{eB}$ is strongly dependent on the B-A/B-X branching ratio. As rough indicators we give the following values of $\Delta\varepsilon$: 375 $cm^{-1}$ for KrCl, -130 $cm^{-1}$ for XeCl, and -70 $cm^{-1}$ for XeBr. Our XeI spectra suffer from impurity problems and have not yet been interpreted quantitatively. We have not yet extended these experiments to the RgF molecules but have no reason to doubt the reversed ordering (i.e. negative $\Delta\varepsilon$) in XeF, which from theoretical considerations is the RgX molecule most likely to show this reversal. From the trends in the results now available for $\Delta\varepsilon$, it seems likely that the C state lies near (within 200 $cm^{-1}$) the B state in KrF, ArF, and possibly XeI and ArCl, but significantly higher than B in the other KrX and ArX molecules.

### B. Halogens

### 1. Overview

The UV emission spectra of the halogens have been the subject of numerous investigations in the last sixty years. (See Refs. 21 and 22 and references cited therein). The spectrum of $I_2$ excited in the presence of foreign gases has proved particularly challenging to spectroscopists. In 1968 Wieland and I began an isotope shift study of this spectrum, which very early corroborated
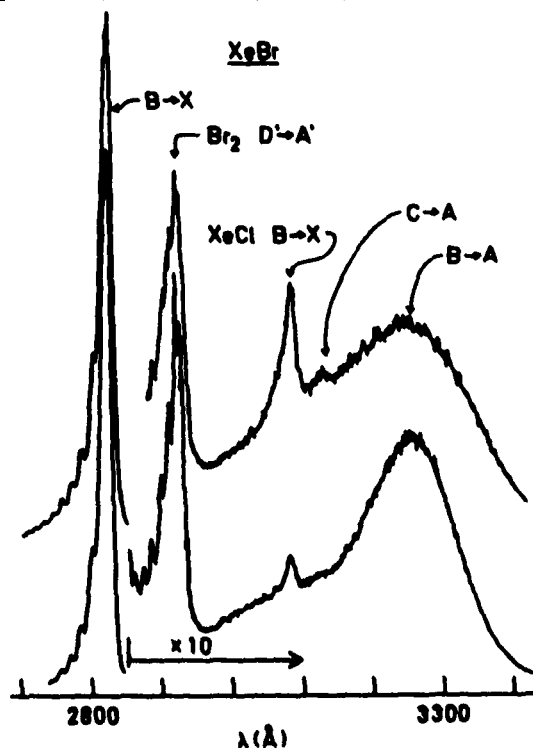
Fig. 8. Emission spectra of XeBr in Ar buffer at P = 700 torr and two temperatures -- 360 K (lower) and 800 K (upper).

the existing analyses of two of the weaker band systems in the spectrum - F → X (2600 A) and E → B (4300 A).[21] In the case of the third and strongest system near 3400 A, the results indicated that all previous analyses were incorrect. However, because this system is quite complicated in certain respects, the full analysis has not yet been finalized and published.

In 1975 the $I_2$ 3400-A emission system came into prominence of a practical nature as several groups predicted[23] and observed[2c,3b,24] lasing on this transition. Subsequently similar experiments with $Br_2$ yielded lasing on the so-called E → B transition near 2900 A.[4b,25] Further work has achieved lasing on transitions in $F_2$ (1580 A),[5c] $Cl_2$ (2580 A),[5d] and ClF (2850 A).[26]

The similarities in the $I_2$ and $Br_2$ laser transitions suggested that the two systems were of the same electronic origin. A re-examination of the $Br_2$ 2900-A system using single isotopes of bromine confirmed that the E → B designation was incorrect and led to the common designation $D'(2g^3\Pi)$ → $A'(2u^3\Pi)$ for these systems in $I_2$ and $Br_2$.[27] According to this assignment the lower state is the lowest excited state in each molecule and dissociates to two ground-state ($^2P_{3/2}$) atoms. The D' state is an ion-pair state which tends toward $X^+(^3P) + X^-(^1S)$ in the asymptotic limit. From its resistance to collisional quenching at high pressures, it seems reasonable that the D' state is the lowest of the ion-pair states. This notion is supported by recent theoretical work,[28,29] but there is some experimental evidence that one or more ion-pair states lie lower than D' in $I_2$.[30,31]

A similar reinvestigation of the 2580-A emission system in $Cl_2$ has found fault with the E → B designation here too. However, we have so far been unable to give a satisfactory analysis for this system, which appears to be heavily perturbed. These observations may tie in with the expected trend toward Hund's case (a) coupling in the lighter halogens, in which event the spectrum is expected to become more complex due to involvement of additional fine structure components of the $^3\Pi$ states. We are unaware of any analyses of the lasing transitions in $F_2$ and ClF.

Figure 9 shows the potential diagram for the $Br_2$ D' → A' transition and indicates the main bands which appear in the laser spectrum. The diagram for $I_2$ is similar, with lasing occurring mainly on the 0-12, 2-15, 3-17, 1-14, and 0-13 bands. In both cases lasing must actually occur on the densely overlapped rotational lines of these and other nearby bands, and in $Br_2$, on the bands of three different isotopic molecules. From the appearance of the

spectra, the lasing transitions in $F_2$, $Cl_2$, and ClF also involve potential curves configured like those in Fig. 9. All of these systems likely involve charge-transfer transitions from large-R ion-pair excited states to weakly bound lower states lying at smaller R. The high gain near the intensity maxima in these spectra is again (as in the RgX systems) attributable to a minimum in the difference potential, $U_{D'}(R) - U_{A'}(R)$; but here the emission from low v' levels is discrete rather than diffuse and yields what spectroscopists have long known as a "head of heads."

## 2. $Br_2$ D' → A' Emission

We have completed our analysis of the D' → A' transition in $Br_2$ and are preparing the results for publication.[32,33] The work includes rotational analyses of 11 v'-v" bands for [79]$Br_2$ and 3 for [81]$Br_2$, plus vibrational assignments for about 50 additional band heads in the spectra of these two isotopic molecules. Virtually every observed spectral feature above 2800 A can be accounted for in terms of this analysis, which means that there is no significant emission from other transitions in this spectral region under the conditions of our emission source (a tesla discharge through 2 torr $Br_2$ and 200 torr Ar).
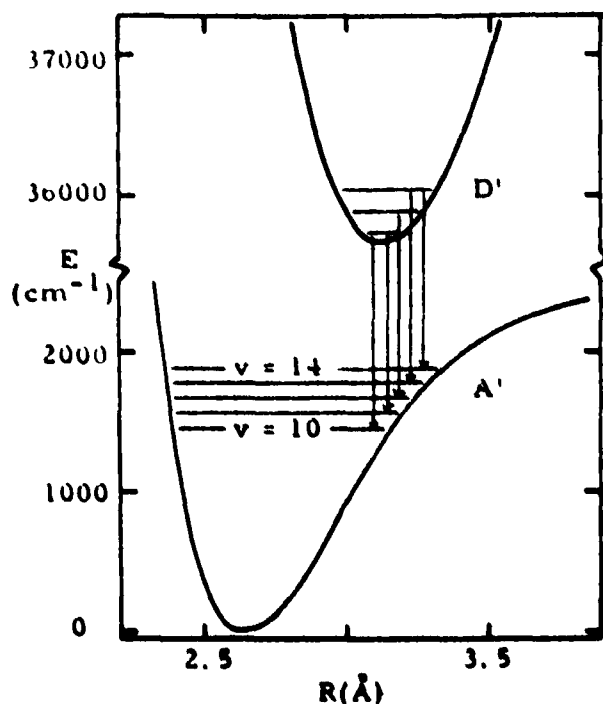


Fig. 9. Potential diagram illustrating main transitions occurring in the $Br_2$ UV laser. Energies are relative to the minimum of the A' curve.

The spectroscopic constants obtained from a least-squares fit of all assigned features are summarized in Table III. The new vibrational constants do not differ significantly form the preliminary values based on band heads alone.[26] Accordingly the $\mathcal{D}_e$ and $T_e$ estimates are little changed. The primary new results of the analysis are the rotational constants, which permit us to determine internuclear distances and calculate reliable potential curves and Franck-Condon factors. The latter are given in Ref. 32. It is worth noting that the internuclear distance in the A' state is close to the known $R_e$ values for the A (1u) and B ($0^+$u) states (2.70 and 2.68 A, respectively[34,35]), which are the other fine structure components of the case (a) $^3\Pi_u$ state. On the other hand the vibrational frequencies vary considerably for the three states: $\omega_{eB}$ = 168 cm$^{-1}$, $\omega_{eA}$ = 154 cm$^{-1}$, and $\omega_{eA'}$ = 165 cm$^{-1}$. In fact both $R_{eA}$ and $\omega_{eA}$ are still not pinned down definitively by our analysis, because the lowest v" level included in the analysis is v" = 5.

### 3. $I_2$ Emission

Work on the $I_2$ D' → A' system near 3400 A is nearing completion. In the meantime we have begun a more extensive study of the emission spectrum of $I_2$ in foreign gases. This work has been spurred on by the recent attribution of a second emission system, near 5000 A, to the same D' state responsible for the 3400-A emission.[36]

Figure 10 shows the emission spectrum of $I_2$ in Ar between 2000 A and 6000 A, as excited by a tesla coil at a pressure of about 1 atm. The D' → A' system is by far the dominant emission under these conditions, but there are a number of weaker systems, some previously analyzed, some not. Among the former are the F → X system near 2600 A and the E → B system near 4300 A. Vibrational structure appears also in the systems near 2380 A, 2480 A, 2780 A, 2860 A, and 3860 A, but remains unanalyzed or a best uncertain.

The broad band near 5000 A shows no discernible fine structure. Our work on the pressure dependence of this band tends to corroborate Hemmati and Collins[36] assignment of this system as originating from the D' state. However, energetic considerations raise doubts about their assignment of the 2u($^3\Delta$) state as the terminus. This 2u state must dissociate to one ground-state and one excited-state I atom,[37] whereas our analysis indicates clearly that the lower state in this system must go to two ground-state atoms. In that case the lower state cannot be a 2u state, since there is only one such state and

TABLE III. Spectroscopic parameters ($cm^{-1}$) for the A' and D' states of $^{79}Br_2$.

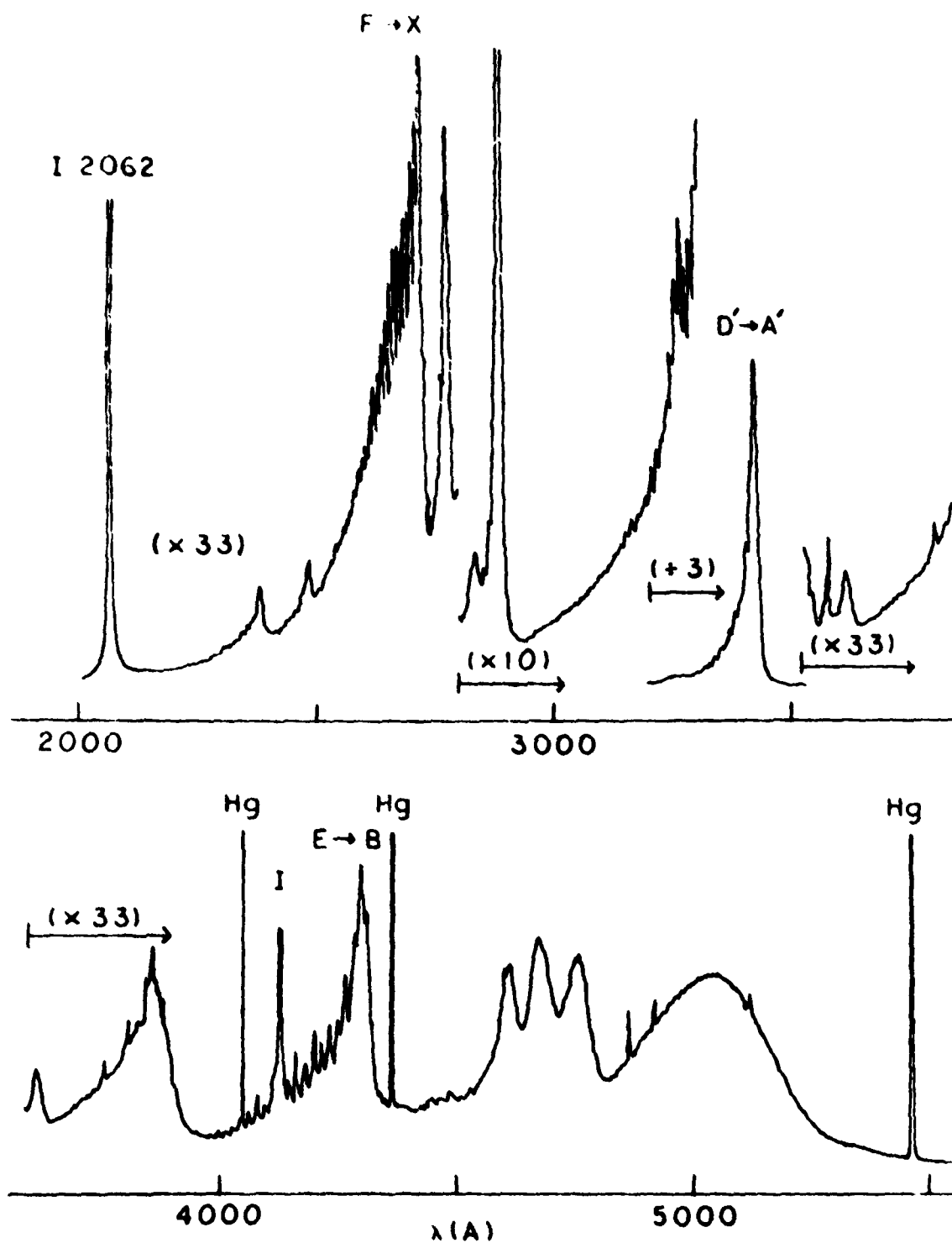| | A' | D' |
|---|---|---|
| $\Delta T_e$ | [35705.97(78)] | |
| $T_e$ | 13240(100) | 48950(100) |
| $C_{v1}(\omega_e)$ | 165.172(379) | 150.863(10) |
| $C_{v2}(-\omega_e x_e)$ | -2.504(71) | -0.3842(14) |
| $C_{v3}$ | 0.0569(64) | |
| $C_{v4}$ | $-4.624(276) \times 10^{-3}$ | |
| $C_{v5}$ | $9.452(456) \times 10^{-5}$ | |
| $D_e$ | 2820(100) | 35540(100) |
| $C_{r1}(B_e)$ | 0.059439(50) | 0.042515(21) |
| $C_{r2}(-\alpha_e)$ | $-5.604(128) \times 10^{-5}$ | $-1.507(16) \times 10^{-5}$ |
| $C_{r3}$ | $-3.568(1160) \times 10^{-6}$ | |
| $C_{r4}$ | $-6.891(342) \times 10^{-7}$ | |
| $R_e(A)$ | 2.6810 | 3.1700 |
| $C_{d1}(D_e)$ | $4.582 \times 10^{-8}$ | $1.351 \times 10^{-7}$ |
| $C_{d2}(\beta_e)$ | $-2.86 \times 10^{-9}$ | $1.33 \times 10^{-11}$ |
| $C_{d3}$ | $3.86 \times 10^{-10}$ | |
| $C_{h1}(H_e)$ | $4.66 \times 10^{-13}$ | |
| $C_{h2}$ | $-1.04 \times 10^{-13}$ | |
| $C_{h3}$ | $7.57 \times 10^{-15}$ | |
| $C_{\ell1}$ | $1.24 \times 10^{-17}$ | |
| $C_{\ell2}$ | $-3.26 \times 10^{-18}$ | |
| $C_{\ell3}$ | $2.27 \times 10^{-19}$ | |
| $\sigma$ | 0.10 | |

Fig. 10. Emission spectrum of $I_2$ in Ar at P = 690 torr, excited with a tesla coil. Note intensity scale changes near 2800 A, 3300 A, and 3500 A.

that one is involved in the 3400 emmission. The most likely candidate for
the lower state then becomes the $3u(^3\Delta)$ state, in which case it is surprising
that the 5000 system is as strong as it is, since as a rule[37] the perpendi-
cular transitions are much weaker than the parallel transitions in $I_2$. One
other possibility is that the 5000-A emission originates not from the D' state
but from a state almost isoenergetic and thermally equilibrated with D'.
We are presently checking on this possibility through careful measurements of
relative emission strength as a function of temperature.

### 4. $I_2$ UV Fluorescence

In connection with work on the McLennan band system as a possible tunable
UV laser,[38] we have reinvestigated the discrete region of the same D → X
fluorescence spectrum at low pressures (~30 mtorr). When $I_2$ absorbs radiation
around 1800 A, the excitation goes mainly to high v' levels (~200) of the D
$(0^+u)$ state. At low pressures this state fluoresces back to the X state and
to a second $0^+g$ state correlating with ground-state atoms. The D → X fluore-
scence is discrete below 2400 A and diffuse (bound-free) from 2400 to 3300 A.
The other D → $0^+g$ system shows diffuse bands between 3500 A and 4800 A.
The diffuse bands above 2400 A constitute the so-called McLennan bands.
Those occurring at 3000 - 3300 A have already been analyzed.[38] However
the analysis lacked quantitative reliability for want of precise knowledge
about the D state and because of uncertainties in the X-state potential
at very high v and large R. Our reanalysis of the D → X discrete fluore-
scence was aimed at reducing these uncertainties.[39]

For the X state our work extended the assignments to v" = 99, which
is about 25 levels beyond the highest level assigned previously by Verma,[40]
and within 50 cm$^{-1}$ of the dissociation limit. Using theoretical methods to
treat centrifugal distortion, we obtained from the data spectroscopic con-
stants which differ significantly from those given earlier by Le Roy,[41]
but which are generally in good agreement with the recent results from
Fourier-transform spectroscopic work on the visible-IR B → X fluorescence
excited by an Ar$^+$ laser.[42] For the D state we obtained reliable rotational
constants for a limited region around v' = 200, from which we should be better
able to deduce the D-state potential curve and the D → X dipole strength
function.

### C. The Tesla Discharge

In most of our spectroscopic work we have utilized a tesla discharge as
our emission source. To excite the discharge we have used commercially

available tesla coils, primarily a model designed for continuous duty (Model BD-20 from Electro-Technic Products Co., Chicago, IL). In recent work we have characterized our tesla discharge with respect to its heavy-body temperature,[43] and its temporal properties and total radiant output.[44]

The light from a tesla discharge emerges in pulses which are somewhat irregular in occurrence and intensity. Using a boxcar integrator we have studied the pulse shapes for typical discharges.[44] The results observed for a nitrogen discharge (Fig. 11) are thought to approximate closely the excitation pulse, whereas pulse shapes obtained for other discharges show broadening and washing out of structure which we attribute to retardation from slow chemistry (in some rare gas halide discharges) or slow excited state decay (OH discharge). For typical discharges the average pulse rate is $10^3$/s. The rare-gas halide discharges are among the strongest we have studied, with average total radiant powers around 5 mW for KrCl and XeCl. About 90% of the emission from the rare gas halide sources occurs in the B-X transition. Rough calculations indicate
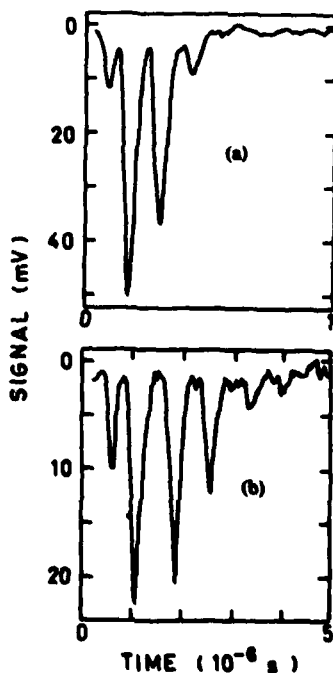


Fig. 11. Pulse shapes for $N_2$ $C \rightarrow B$ emission at 3371 Å, excited in air at 14 Torr pressure by (a) Model BD-20 and (b) Model BD-10 tesla coils. The photomultiplier gain was higher by a factor of 5 for (b) than for (a).

that the peak pulse power of 10 W is within an order of magnitude of that
required to achieve lasing in a small capillary discharge device.

In recording spectra we measure an average DC photocurrent while scanning
the monochromator wavelength. With the exception of the rare gas fluoride
systems, the discharge intensity is stable over times much longer than re-
quired to record a spectrum. However the source is noisy in the short time
regime, so a large capacitor is used to smooth the signal. Also, pulse-forming
capacitors are needed in the PMT circuitry to avoid nonlinearity from saturation
effects associated with the intense pulses.

Studies of the OH A → X emission produced in a tesla discharge indicate
that the discharge can be characterized by a heavy-body temperature only a
few degrees greater than the wall temperature.[43] These results were obtained
by analyzing rotational population distributions in the level v' = 0 of the
A state. Typical Boltzmann-type plots are shown for two different wall tem-
peratures in Fig. 12. By least-squares fitting such data to low-order
polynomials and using the linear coefficients to determine a temperature, we
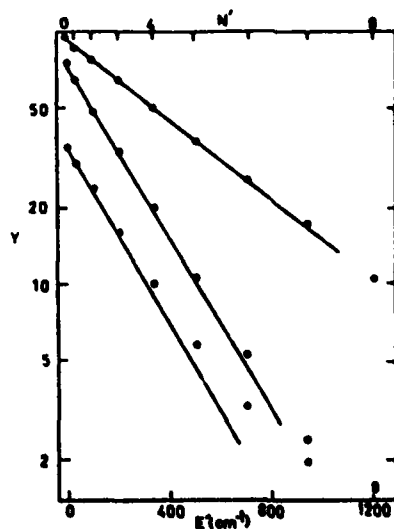conclude that we obtain meaningful heavy-body temperatures for the discharge.



Fig. 12.

Logarithmic plots of Y vs E' and N' from OH A→X emission intensities measured for an argon
Tesla discharge operated at room temperature (lower two) and 486 C (top). Argon pressures were 110 torr
(bottom), 650 torr (middle), and 300 torr (top). Most plotted points are averages of two or three values,
which were too close together to show individually on the scale of this display. The straight lines represent
the linear terms from quadratic least-squares fits and give (bottom to top) T = 356, 367, and 754 K.

To study the temperature dependence of the rare-gas halide emissions, we use the simple oven arrangement illustrated in Fig. 13. The discharge cell is attached directly to a grease-free vacuum line and is isolatable from the line by a greaseless stopcock. Temperatures are measured with iron-constantan thermocouples. The mixing bulb E comprises the bulk of the volume of the discharge cell and is designed to ensure that compositions in the discharge tube are the same as those admitted to the cell at large.

## III. CONCLUSION

The work performed under this contract has led to a detailed spectroscopic description of the UV lasing transitions in several of the RgX molecules and the $X_2$ molecules. In particular we have completed the first rotational and vibrational analyses of the B → X transition in XeF and the D' → A' system in $Br_2$, the first vibrational analyses of the D → X system in XeF, the B → X and D → X systems in XeCl, and the D' → A' transition in $I_2$, and a detailed
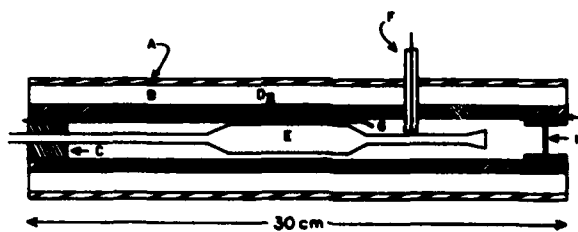


Fig. 13. Cross-sectional view of discharge cell and oven assembly, showing outer Al foil skin (A), asbestos tape insulation (B) and end plug (C), heating tape (D), silica discharge tube and mixing bulb (E), Pyrex capillary feedthrough and tesla electrode (F), iron-constantan thermocouple (G), silica window in asbestos ring mounts (H), and Pyrex sheath (I).

reanalysis of the D → X fluorescence spectrum in $I_2$. In addition we have expanded on our earlier first quantitative treatment of the B → X and D → X structured continua which occur in the emission spectra of most of the RgX molecules, and have determined the energy ordering of the C and B states in several of these molecules. In an aside, we have characterized our tesla discharge with respect to its temporal and thermal behavior and its total radiant output.

Work remains incomplete in several of these areas. Specifically, additional work is needed on (1) the rotational analysis of the B → X and D → X systems in $^{136}Xe^{19}F$; (2) the dipole strength function for the B-X system of XeF; (3) the bound-free structured continua in XeBr, XeI, KrF, KrBr, ArF, ArCl, and ArBr at high pressures; (4) vibrational relaxation in KrCl and XeF; (5) energy ordering of the B and C states in the RgF molecules; (6) analysis of the lasing transitions in $Cl_2$, $F_2$, and ClF; and (7) further work on the emission and fluorescence spectra of the halogens. We are currently seeking financial support to continue this work.

## IV. REFERENCES

1. S. K. Searles and G. A. Hart, Appl. Phys. Lett. **27**, 243 (1975).

2. (a) J. J. Ewing and C. A. Brau, Appl. Phys. Lett. **27**, 350 (1975;
   (b) C. A. Brau and J. J. Ewing, ibid. 435 (1975);
   (c) J. J. Ewing and C. A. Brau, ibid. 557 (1975).

3. (a) E. R. Ault, R. S. Bradford, Jr. and M. L. Bhaumik, Appl. Phys. Lett. **27**, 413 (1975);
   (b) R. S. Bradford, Jr., E. R. Ault and M. L. Bhaumik, ibid. 546 (1975).

4. (a) J. R. Murray and H. T. Powell, Appl. Phys. Lett. **29**, 252 (1976);
   (b) J. R. Murray, J. C. Swingle and C. E. Turner, Jr., ibid. **28**, 530 (1976).

5. (a) G. C. Tisone, A. K. Hays and J. M. Hoffman, Opt. Comm. **15**, 188 (1975);
   (b) J. M. Hoffman, A. K. Hays and G. C. Tisone, Appl. Phys. Lett. **28**, 538 (1976);
   (c) J. K. Rice, A. K. Hays and J. R. Woodworth, ibid. **31**, 31 (1977).
   (d) A. K. Hays, Opt. Comm. **28**, 209 (1979).

6. R. W. Waynant, Appl. Phys. Lett. **28**, 538 (1977).

7. (a) J. Tellinghuisen, G. C. Tisone, J. M. Hoffman and A. K. Hays, J. Chem. Phys. **64**, 4796 (1976).
   (b) J. Tellinghuisen, J. M. Hoffman, G. C. Tisone and A. K. Hays, ibid. 2484 (1976);
   (c) J. Tellinghuisen, A. K. Hays, J. M. Hoffman and G. C. Tisone, ibid. **65**, 4473 (1976).

8. (a) T. H. Dunning, Jr. and P. J. Hay, Appl. Phys. Lett. **28**, 649 (1976);
   (b) P. J. Hay and T. H. Dunning, Jr., J. Chem. Phys. **66**, 1306 (1977);
   (c) T. H. Dunning, Jr. and P. J. Hay, ibid. **69**, 134 (1978);
   (d) P. J. Hay and T. H. Dunning, Jr., ibid. 2209 (1978).

9. (a) J. Tellinghuisen, P. C. Tellinghuisen, G. C. Tisone, J. M. Hoffman and A. K. Hays, J. Chem. Phys. **68**, 5177 (1978);
   (b) P. C. Tellinghuisen, J. Tellinghuisen, J. A. Coxon, J. E. Velazco and D. W. Setser, J. Chem. Phys. **68**, 5187 (1978).

10. D. Kligler, H. H. Nakano, D. L. Huestis, W. K. Bischel, R. M. Hill and C. K. Rhodes, Appl. Phys. Lett. **33**, 39 (1978).

11. (a) J. H. Kolts and D. W. Setser, J. Phys. Chem. **82**, 1766 (1978);
    (b) H. C. Brashears and D. W. Setser, Appl. Phys. Lett. **33**, 821 (1978);
    (c) H. C. Brashears and D. W. Setser, J. Phys. Chem. (submitted).

12. G. Black, R. L. Sharpless, D. C. Lorents, R. Gutcheck, T. Bonifeld, D. Helms, and G. K. Walters (to be published).

13. J. Tellinghuisen and M. R. McKeever (to be published).

14. A. Sur, A. K. Hui and J. Tellinghuisen, J. Mol. Spectrosc. **74**, 465 (1979).

15. M. Shimauchi, S. Karasawa and T. Miura, J. Chem. Phys. **68**, 5657 (1978).

16. J. E. Velazco and D. W. Setser, J. Chem. Phys. **62**, 1990 (1975).

17. J. J. Ewing and C. A. Bran, Phys. Rev. A **12**, 129 (1975).

18. M. R. McKeever, M. B. Moeller and J. Tellighuisen (to be published).

19. M. Krauss and B. Liu, Chem. Phys. Lett. 44, 257 (1976).

20. P. C. Tellinghuisen and J. Tellinghuisen (to be published).

21. K. Wieland, J. B. Tellinghuisen and A. Nobs, J. Mol. Spectrosc. 41, 69 (1972).

22. R. S. Mulliken, J. Chem. Phys. 55, 288 (1971).

23. M. V. McCusker, R. M. Hill, D. L. Huestis, D. C. Lorents, R. A. Gutcheck and H. H. Nakano, Appl. Phys. Lett. 27, 363 (1975).

24. A. K. Hays, J. M. Hoffman and G. C. Tisone, Chem. Phys. Lett. 39, 353 (1976).

25. J. J. Ewing, J. H. Jacob, J. A. Mangano and H. A. Brown, Appl. Phys. Lett. 28, 656 (1976).

26. M. Diegelmann, K. Hohla, and K. L. Kompa, Optics Comm. 29, 334 (1979).

27. J. Tellinghuisen, Chem. Phys. Lett. 49, 485 (1977).

28. G. Das and A. C. Wahl, J. Chem. Phys. 69, 53 (1978).

29. R. L. Jaffe, to be published (private communication).

30. M. D. Danyluk and G. W. King, Chem. Phys. 22, 59 (1977).

31. K. K. Lehmann, J. Smolarek and L. Goodman, J. Chem. Phys. 69, 1569 (1978).

32. A. Sur, Ph.D. Thesis, Vanderbilt University (1980).

33. A. Sur and J. Tellinghuisen (to be published).

34. R. F. Barrow, T. C. Clark, J. A. Coxon and K. K. Yee, J. Mol. Spectrosc. 51, 428 (1974).

35. J. A. Coxon, J. Mol. Spectrosc. 41, 566 (1972).

36. H. Hemmati and G. J. Collins, Chem. Phys. Lett. 67, 5 (1979).

37. R. S. Mulliken, J. Chem. Phys. 55, 288 (1971).

38. J. Tellinghuisen, Chem. Phys. Lett. 29, 359 (1974).

39. J. Tellinghuisen, M. R. McKeever and A. Sur, J. Mol. Spectrosc. (in press).

40. R. D. Verma, J. Chem. Phys. 32, 738 (1960).

41. R. J. LeRoy, J. Chem. Phys. 52, 2683 (1970).

42. R. Bacis, S. Churassy, R. W. Field, J. B. Koffend and J. Verges (to be published).

43. A. K. Hui, M. R. McKeever and J. Tellinghuisen, J. Quant. Spectros. Radiat. Transfer 21, 387 (1979).

44. M. R. McKeever, A. Sur, A. K. Hui and J. Tellinghuisen, Rev. Sci. Instrum. 50, 1136 (1979).

## V. APPENDIX A. PUBLICATIONS AND PRESENTATIONS

1. "Pressure Dependence of the KrF B+X Spectrum," By Amit K Hui and Joel Tellinghuisen, contributed talk presented June 17, 1977 at the 32nd Symposium on Molecular Spectroscopy (Ohio State University, Columbus, Ohio).

2. "Intensity Factors for the $I_2$ B↔X Band System," by Joel Tellinghuisen, J. Quant. Spectrosc. Radiat. Transfer 19, 149 (1978).

3. "Spectroscopic studies of diatomic noble gas halides. III. Analysis of XeF 3500 Å band system," by Joel Tellinghuisen, Patricia C. Tellinghuisen, G. C. Tisone, J. M. Hoffman, and A. K. Hays, J. Chem. Phys. 68, 5177 (1978).

4. "Spectroscopic studies of diatomic noble gas halides. IV. Vibrational and rotational constants for the X, B, and D states of XeF," by Patricia C. Tellinghuisen, Joel Tellinghuisen, J. C. Coxon, J. E. Velazco, and D. W. Setser, J. Chem. Phys. 68, 5187 (1978).

5. "Analysis of the UV Laser Transition in $Br_2$," by Abha Sur and Joel Tellinghuisen, contributed talk presented June 14, 1978 at the 33rd Symposium on Molecular Spectroscopy (Ohio State University, Columbus, Ohio).

6. "The B+X and D+X Systems of XeCl," by Amit K. Hui, Abha Sur, and Joel Tellinghuisen, contributed talk presented June 14, 1978 at the 33rd Symposium on Molecular Spectroscopy (Ohio State University, Columbus, Ohio).

7. "The B+X System of KrCl," by Mark R. McKeever, Joel Tellinghuisen, and Michael B. Moeller, contributed talk presented June 14, 1978 at the 33rd Symposium on Molecular Spectroscopy (Ohio State University, Columbus, Ohio).

8. "Noble Gas Halides. The B+X and D+X Systems of $^{136}Xe^{35}Cl$," by Abha Sur, Amit K. Hui, and Joel Tellinghuisen, J. Mol. Spectrosc. 74, 465 (1979).

9. "Temperatures of Tesla Discharges from OH A+X Intensity Measurements," by Amit K. Hui, Mark R. McKeever, and Joel Tellinghuisen, J. Quant. Spectrosc. Radiat. Transfer 21, 387 (1979).

10. "The tesla discharge as a spectroscopic source for the study of excimer laser transitions," by Mark R. McKeever, Abha Sur, Amit K. Hui, and Joel Tellinghuisen, Rev. Sci. Instrum. 50, 1136 (1979).

11. "Reanalysis of the D+X Fluorescence Spectrum of $I_2$," by Joel Tellinghuisen, Mark R. McKeever, and Abha Sur, J. Mol. Spectros. (in press).

12. "Spectroscopy with a Tesla Coil," by Mark R. McKeever, Abha Sur, Amit K. Hui, and Joel Tellinghisen, contributed talk presented at the 34th Symposium on Molecular Spectroscopy (Ohio State University, Columbus, Ohio), June, 1979.

13. "Re-examination of the Discrete Region of the UV Fluorescence System D+X in $I_2$," by Abha Sur, Mark R. McKeever, and Joel Tellinghuisen, contributed talk presented at the 34th Symposium on Molecular Spectroscopy (Ohio State University, Columbus, Ohio), June, 1979.

14. "Spectroscopic Studies of Rare Gas Halides," by Joel Tellinghisen, invited talk presented at a Topical Meeting on Excimer Lasers sponsored by the IEEE and the Optical Society of America (Charleston, South Carolina), September, 1979.

15. "Energy Ordering of the B and C States in KrCl, XeCl, and XeBr from Temperature Dependence of Emission Spectra," by Joel Tellinghuisen and Mark R. McKeever, Chem. Phys. Lett. (to be submitted).

16. "Analysis of bound-free emission spectra of KrCl," by Mark R. McKeever, Michael B. Moeller, and Joel Tellinghuisen, J. Chem. Phys. (to be submitted).

17. "Rotational Analysis of the D'→A' System (2900 A) in $Br_2$," by Abha Sur and Joel Tellinghuisen, J. Mol. Spectrosc.(to be submitted).